JOPSS
JAEA Originated Papers Searching System

日本原子力研究開発機構機関リポジトリ
Japan Atomic Energy Agency Institutional Repository

Title	Analyses of $H^*(10)$ dose rates measured in environment contaminated by radioactive caesium; Correction of directional dependence of scintillation detectors
Author(s)	Tsuda Shuichi, Tanigaki Minoru, Yoshida Tadayoshi, Okumura Ryo, Saito Kimiaki
Citation	Radiation Protection Dosimetry, 193(3-4), p.228-236
Text Version	Published Journal Article
URL	https://jopss.jaea.go.jp/search/servlet/search?5070693
DOI	https://doi.org/10.1093/rpd/ncab060
Right	© The Author(s) 2021. Published by Oxford University Press. All rights reserved.

Japan Atomic Energy Agency

Radiation Protection Dosimetry (2021), Vol. 193, No. 3–4, pp. 228–236 doi:10.1093/rpd/ncab060
Advance Access publication 24 April 2021

ANALYSES OF $H^*(10)$ DOSE RATES MEASURED IN ENVIRONMENT CONTAMINATED BY RADIOACTIVE CAESIUM: CORRECTION OF DIRECTIONAL DEPENDENCE OF SCINTILLATION DETECTORS

S.Tsuda[1,*], M. Tanigaki[2], T. Yoshida[3], R. Okumura[2] and K. Saito[4]
[1]Research group for radiation transport analysis, Japan Atomic Energy Agency, 2-4, Shirakata, Tokai-mura, Naka-gun, Ibaraki 319-1195, Japan
[2]Institute for Integrated Radiation and Nuclear Science, Kyoto University, 2, Asashiro-Nishi, Kumatori-cho, Sennan-gun, Osaka 590-0494, Japan
[3]Emergency Administration Section, Japan Atomic Energy Agency, 765-1 Funaishikawa, Tokai-mura, Naka-gun, Ibaraki 319-1184, Japan
[4]Sector of Nuclear Safety Research and Emergency Preparedness, Japan Atomic Energy Agency, 148-4 Kashiwanoha Campus,178-4 Wakashiba, Kashiwa-city, Chiba, 277-0871, Japan

*Corresponding author: tsuda.shuichi@jaea.go.jp

Received 2 February 2021; revised 8 March 2021; editorial decision 1 April 2021; accepted 1 April 2021

Ambient dose equivalent rates were measured in the environment of the Fukushima prefecture using NaI(Tl)/CsI(Tl) scintillation detectors and CdZnTe/Ge semiconductor detectors. The dose rates obtained at the same locations varied beyond uncertainty (1σ). By replacing the spectrum-dose conversion operators obtained from the anterior–posterior geometry with those from the rotational geometry, the dose rates agreed with each other within uncertainties, except for a CsI(Tl) scintillation detector with a considerably flat crystal configuration, due to its excessive directional dependence.

INTRODUCTION

The Great East Japan Earthquake, on 11 March 2011, provoked the release of large amounts of radionuclides into the environment from the Fukushima Daiichi Nuclear Power Plant (FDNPP)[(1)]. The Japan Atomic Energy Agency (JAEA) has been conducting environmental radiation monitoring of soil and river/sea water and dose rate mapping.

Soon after the accident, the Kyoto University RAdiation MApping system (KURAMA[(2)]) was developed using a conventional NaI(Tl) survey metre and started significantly contributing to the efficient collection of ambient dose equivalent ($H^*(10)$) rates. However, NaI(Tl) survey metres were originally intended for nuclear power plants or radioisotopes facilities and are not specialised for environmental monitoring; this is also the case for the kinds of scintillation detectors[(3–5)] that became available after the accident and used for the environmental measurement.

The KURAMA system has been improved as KURAMA-II[(6–8)], specifically in compactness and autonomous operation using CsI(Tl) scintillation detectors[(3)]. In parallel with practical operations, studies on environmental dose rate monitoring are ongoing. For insights into the directional dependence of the CsI(Tl) scintillation detectors installed in KURAMA-II, response functions and spectrum-dose conversion operators ($G(E)$ functions[(9)]) were determined[(10)] under a virtual accident environment where caesium isotopes exist on the soil surface. The simulation revealed that the dose rates measured in the environment could depend on the detector's crystal configuration. For an experimental confirmation of the influence of such configuration, pulse height spectra were measured[(11)] in several locations in Fukushima by using several kinds of scintillation detectors[(2)] with different crystal configurations and the dose rates were compared. Some results related to KURAMA-II have been reported elsewhere[(11)], but others were also worth further general discussion with regard to the directional dependence of $H^*(10)$ rate measurement in the environment.

In this paper, $H^*(10)$ rates measured outside using six detectors with different crystal configurations were reported and correction of $H^*(10)$ values and its limitation are discussed.

MATERIALS AND METHODS

Locations of measurement in Fukushima

Pulse height spectra were measured in the six locations shown in Figure 1. The places labelled Nos. 4–6 were relatively open, flat and ideal for *in situ*

© The Author(s) 2021. Published by Oxford University Press. All rights reserved. For Permissions, please email: journals.permissions@oup.com

Downloaded from https://academic.oup.com/rpd/article/193/3-4/228/6248462 by Japan Atomic Energy Agency user on 16 August 2021

Figure 1: Measurement locations in Fukushima.

dose rate measurement. The places marked Nos. 1–3 were comparatively close to the sea or mountains. The farthest site (No. 1) was located ∼25 km away from the FDNPP. The condition of No. 6 is presented in Figure 2. Before determining the places where the dose rate measurements were to be conducted, we ensured that there was no significant variation in the dose rate in every area because detectors cannot be installed in the exact same place, as shown in Figure 2. The stands used to install the detectors were made of thin stainless-steel mesh to lessen shielding effects. The weather condition was almost stable throughout the measurements.

In addition to the suitability of the physical conditions for the *in situ* measurements, the dose rate level was considered in selecting the measurement areas to avoid significant counting loss of the detectors. Considering the difference in detection efficiencies among the instruments, measurements were performed in 30 or 60 min at each site to ensure that the statistical fluctuations in the pulse height spectra were $<1\%$ for the mixed peak counts of 796 and 802 keV for ^{134}Cs, 605 keV for ^{134}Cs and 662 keV for ^{137}Cs, although counts for natural radionuclides, such as ^{40}K and ^{214}Bi were not always sufficient.

Figure 2: Detectors' setting in the location No. 6.

Detectors

Table 1 presents the detector specifications used in this study. Three types of CsI(Tl) scintillation

Downloaded from https://academic.oup.com/rpd/article/193/3-4/228/6248462 by Japan Atomic Energy Agency user on 16 August 2021

Table 1. The geometry parameters of the crystals in the detectors taken in this study.

Detector name	Crystal type	Crystal size (mm)	Crystal volume (mm^3)
C12137-00		$13 \times 13 \times 20$	3.4×10^3
C12137-01	CsI(Tl)	$38 \times 38 \times 25$	3.6×10^4
C12137-10		$110\phi \times 25$	2.4×10^5
TCS-161	NaI(Tl)	$25.4\phi \times 25.4$	1.3×10^4
GR1	CdZnTe	$10 \times 10 \times 10$	1.0×10^3
Falcon 5000	Ge	$60\phi \times 30$	8.5×10^4

detectors[3] were used and all were manufactured by HAMAMATSU Photonics K. K. The CsI(Tl) crystals are rectangular parallelepipeds sized $13 \times 13 \times 20\ mm^3$ (C12137-00) and $38 \times 38 \times 25\ mm^3$ (C12137-01). C12137-10 has a cylindrical CsI(Tl) crystal with $110\phi \times 25$ mm height. Due to the large crystal size of C12137-10, which is ~10 times that of the TCS-161 survey metre (Hitachi, Ltd), it can detect the contributions of natural nuclides at high rates, while excessive counting losses >50% were observed at some locations.

C12137-00 or C12137-01 were incorporated in KURAMA-II[6–8]. Thus, the indicated values of $H^*(10)$ and pulse height spectra were obtained every 3 s through the communication line of KURAMA-II via the Internet, whereas the data of C12137-10 were directly sent to a laptop PC to store the pulse height spectra data. C12137-10 has a flat crystal suitable for radioactivity measurement, and its shape was suitable for this study's investigation of the directional characteristics of various scintillation detectors.

A TCS-161 survey metre was also used; it is equipped with a $25.4\phi \times 25.4$ mm-height cylindrical NaI(Tl) scintillation crystal in the probe. The probe was connected to a multichannel analyser[12] and a laptop PC to store the pulse height spectra data. The probe specifications of TCS-161 are equivalent to those of TCS-172B.

For GR1[13], manufactured by Kromek, its CdZnTe crystal is a right cube sized $1\ cm^3$. The energy resolution is ~2% in the full width at half maximum (FWHM) for 662 keV gamma ray from ^{137}Cs and superior to that of inorganic scintillation detectors, but its detection sensitivity is lower than that of other detectors due to its small crystal size. The pulse height spectra from GR1 were collected using a laptop PC.

High-purity germanium (HPGe) detectors have been widely used for *in situ* measurement after the FDNPP accident to investigate the spatial distributions of radionuclides deposited onto ground soil[15]. For a comparison of *in situ* measurement techniques, the portable HPGe detector Falcon 5000[14] (Mirion Technologies, Inc.) was used. The cylindrical Ge crystal measures 60 mm in diameter and 30 mm in height. The cylindrical base was facing the ground surface during the measurement.

Table 2. Gamma ray sources used for energy calibration

Radioisotope sources or Materials	Emitted gamma-ray energy (keV)
^{241}Am	59.5
^{133}Ba	81, 356
^{57}Co	122
^{137}Cs	662
^{60}Co	1173, 1333
KCl	1461
Uranium rock	609, 1120, 1764, 2204, 2615*

*For C12137-01, C12137-10 and GR1.

Energy calibration

Some gamma-ray sources were used for the energy calibration, as shown in Table 2, to correctly detect natural radionuclides, such as the ^{40}K, ^{238}U and ^{232}Th series existing in the soil, in addition to artificial radionuclides, such as ^{134}Cs and ^{137}Cs.

Pulse height was converted to gamma-ray energy with second-order fitting functions. For C12137-01, C12137-10 and GR1, a peak channel of 2615 keV gamma rays from a uranium rock source was applied when the fitting functions were created.

Dose rate calibration

Dose rate calibrations were performed at the Instrument Calibration Facility in JAEA. The shadow shield technique was performed using a standard ^{137}Cs gamma-ray source (Japan Radioisotope Association, Model 461). Each calibration factor of the detectors was obtained as a ratio of an indicated value by the primary gamma ray from the source to the standard dose rate, except the contributions from the

Downloaded from https://academic.oup.com/rpd/article/193/3-4/228/6248462 by Japan Atomic Energy Agency user on 16 August 2021

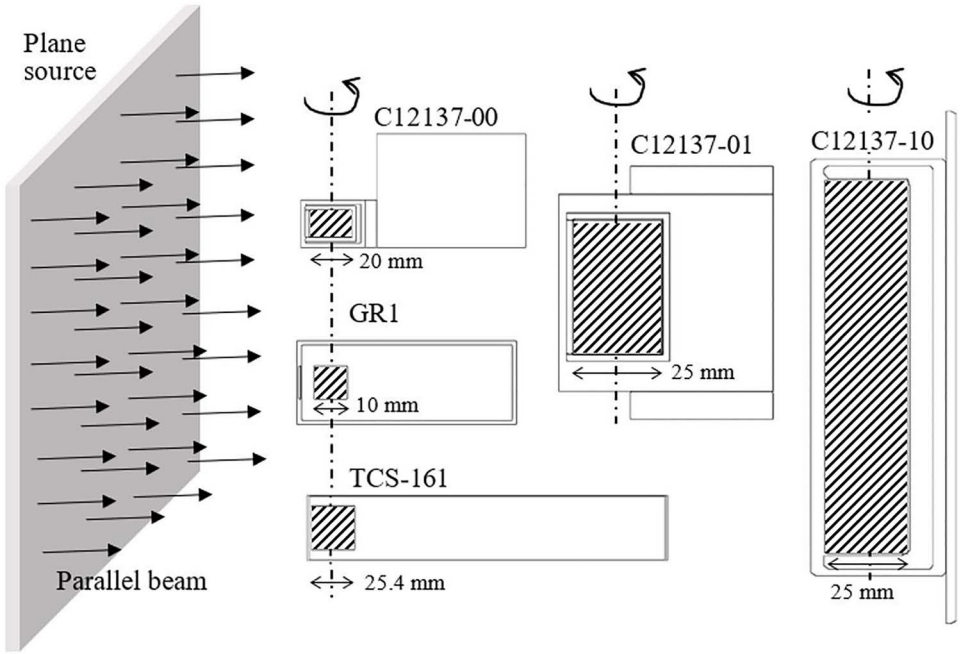

Figure 3: Irradiation geometries of the detectors for the calculation of pulse height spectra (not in scale). Each crystal is highlighted with diagonal lines and its depth length is shown.

scattered gamma rays. With regard to the alignment of the detectors C12137-00, C12137-01 and GR1 with the source, the square surfaces faced the source. For the detectors with cylindrical crystals, the cylindrical bases were vertically turned to the source.

G(*E*) function

For C12137-00, C12137-01 and TCS-161, the $H^*(10)$ dose rates were obtained by multiplying the $G(E)$ functions[10,16] with the measured pulse height spectra. For C12137-10 and GR1, the $G(E)$ functions were newly determined by the conversion coefficients[17] from the photon fluence to $H^*(10)$ and 16 datasets of pulse height distributions of mono-energetic gamma rays from 40 keV to 3,000 keV, as calculated by the PHITS[18] code. The calculation geometries of the pulse height spectra are presented in Figure 3; details about the calculation are available elsewhere[7,8,10,16]. Hereafter, the parallel beam irradiation geometry is named anterior–posterior irradiation geometry (AP). The arrows around the central axes of the crystals in Figure 3 indicate the rotational direction when the detectors are irradiated in the rotational irradiation geometry (ROT).

The $G(E)$ functions in AP are shown in Figure 4. The overall shapes appear similar, but the values increase with decreasing crystal volume because the number of detected gamma rays increases with the crystal volume.

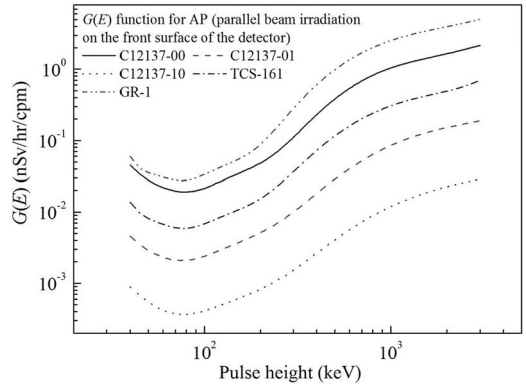

Figure 4: G(E) functions determined by parallel beam irradiation on the front surface of the detectors.

Data analysis of Ge detector

For the Falcon 5000, the dose rates were deduced by the conversion factors[19] from the radioactivity to $H^*(10)$ of each nuclide, according to the method stated in ICRU Report No. 53[20] for environmental

Downloaded from https://academic.oup.com/rpd/article/193/3-4/228/6248462 by Japan Atomic Energy Agency user on 16 August 2021

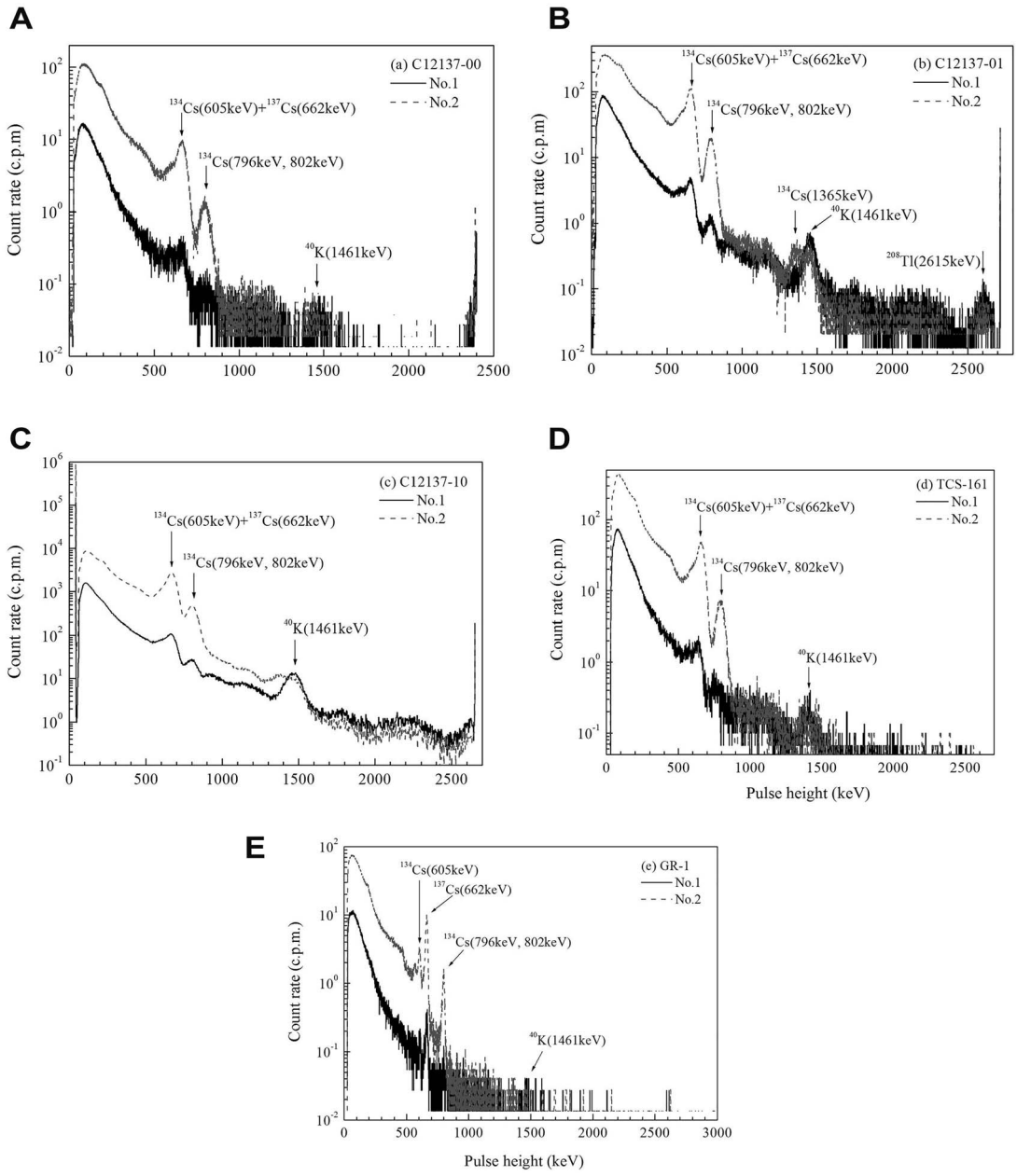

Figure 5: Pulse–height distributions measured by: (a) C12137-00, (b) C12137-01, (c) C12137-10, (d) TCS-161(lateral). Pulse height distributions measured in the field by: (e) GR1.

dose monitoring using Ge detectors. The assumed value of relaxation mass depth in the method was 3.13, which was estimated from a series of environmental studies[21] performed in Fukushima prefecture. Therefore, these dose rates were regarded as reference values in this study.

Setting direction

TCS-161 and C12137-10 were set in two directions. The central axes were set in parallel and vertical to the ground to investigate the directional dependence of the detectors on the indicated dose rates.

Downloaded from https://academic.oup.com/rpd/article/193/3-4/228/6248462 by Japan Atomic Energy Agency user on 16 August 2021

Table 3. $H^*(10)$ rates in μSv/h measured in Fukushima prefecture.

Place	C12137-00	C12137-01	GR1	Falcon 5000
No.1	0.257	0.204	0.243	0.256
No.2	2.64	1.76	2.464	4.52
No.3	0.227	0.168	0.194	0.264
No.4	0.689	0.507	0.646	0.954
No.5	2.94	1.89	2.882	5.05
No.6	0.235	0.188	0.211	0.214
Place	TCS-161 lat.	down.	C12137-10 lat.	up.
No.1	0.236	0.231	0.191	0.178
No.2	2.16	2.19	3.04	2.75
No.3	0.204	0.212	0.163	0.150
No.4	0.599	0.612	0.556	0.507
No.5	2.32	2.39	3.25	2.93
No.6	0.239	0.244	0.191	0.179

Table 4. Ratios of $H^*(10)$ rates measured laterally to those vertically.

Place	TCS-161 lat./down.	C12137-10 lat./up.
No.1	1.02	1.08
No.2	0.99	1.14
No.3	0.96	1.09
No.4	0.98	1.10
No.5	0.97	1.14
No.6	0.98	1.07
Average	0.98 ± 0.02	1.10 ± 0.03

RESULTS AND DISCUSSIONS

Pulse height spectra

The pulse height spectra measured at site Nos. 1 and 2 are presented in Figure 5. These results are presented up to ~2500–3000 keV in pulse height, depending on the detectors. In Figure 5(a), for C12137-00, complex peaks of 605 keV from ^{134}Cs and 662 keV from ^{137}Cs are found between 600 and 700 keV, as well as complex peaks of 796 and 802 keV from ^{134}Cs. The sharp peak around 2400 keV indicates a sum peak due to the over-range signals and the contributions were included in the dose rate. The same procedures were applied to the other data analyses.

The pulse height spectra in Figure 5(b) present the peaks more clearly than those of C12137-00. In the case of No. 2, the peaks of 1365 keV from ^{134}Cs are distinguishable from those of 1460 keV from ^{40}K. Contributions of ^{208}Tl can be seen at ~2600 keV. The peak around 2700 keV is due to the ADC over-range.

C12137-10 has the highest detection sensitivity among the C12137s because it has the largest crystal volume, which is ~70 times that of C12137-00, but its energy resolution is less than those of C12137-00 or C12137-01.

For the results of TCS-161, which are set laterally in Figure 5(d), there are complex peaks from 600 keV to 800 keV from ^{134}Cs and ^{137}Cs, but the contributions of natural nuclides are not as clearly detected by C12137-00.

About the results of GR1 in Figure 5(e), the peaks of 662 keV from ^{137}Cs and 605 keV from ^{134}Cs are clearly distinguished, but their counting rates are the smallest among all detectors due to its small crystal size.

Dose rates

Table 3 shows the dose rates measured in the environment. The possible causes and statistical uncertainties of the indicated values of $H^*(10)$ are as follows: counts of measured pulse height spectra (0.03–0.3%), dose rate calibrations (0.1–1.4%). The systematic uncertainties are attributed to energy calibrations (1–11%), compensation of counting loss (1–15%), introduction of $G(E)$ functions (1–2%) and the experimental settings (5–10%). The uncertainties related to the determination of $G(E)$ functions are based on the $H^*(10)$ dose folding calculations by multiplying each calculated pulse height spectrum for mono-energetic gamma rays from 40 keV to 3000 keV with $G(E)$ functions.

The one standard deviation (1σ) of the overall uncertainties is estimated to be 5.3–10.9% for C12317-00, C12137-01 and TCS-161. For C12137-10, the 1σ value is 18.3%, since the uncertainty of counting loss compensation is 15% at the maximum due to its high detection sensitivity. In the case of GR1, the uncertainty of dose rate calibration is

Downloaded from https://academic.oup.com/rpd/article/193/3-4/228/6248462 by Japan Atomic Energy Agency user on 16 August 2021

Table 5. Ratios of $H^*(10)$ rate of TCS-161 (lat.) to those of other detectors.

Place	C12137-00	C12137-01	C12137-10		GR1	Falcon 5000
			lat.	up.		
No.1	1.09	0.86	0.81	0.75	1.03	1.09
No.2	1.22	0.81	(1.41)	(1.27)	1.14	(2.10)
No.3	1.11	0.82	0.80	0.73	0.95	1.29
No.4	1.15	0.85	0.93	0.85	1.08	1.59
No.5	1.27	0.82	(1.40)	(1.26)	1.24	(2.18)
No.6	0.98	0.79	0.80	0.75	0.88	0.90
Average	1.14	0.83	0.83*	0.77*	1.06	1.22*
	±0.09	±0.03	±0.05	±0.04	±0.12	±0.26

*The values of no.2 and no.5 are not included.

11%, which is larger than the others, and its 1σ is 15.4%.

Directional dependences

The ratios of the $H^*(10)$ rates measured laterally to those measured vertically are presented in Table 4. For TCS-161, the ratio is 0.98 ± 0.02; this indicates[11] that TCS-161 has a relatively small angular dependence, mainly due to its right cylindrical crystal configuration.

For C12137-10, the ratio is 1.10 ± 0.03. Since C12137-10 has a rather flat and large effective crystal surface where gamma rays can reach specifically when it is set laterally, the dose rates in the lateral setting are higher than those in the upward positioning, but the difference seems fairly small given the aspect ratio of the crystal. This result is consistent with a previous result[22] stating that the gamma-ray fluence in the lateral direction is dominant in environments where gamma-ray-emitting radionuclides exist in the surface soil.

Differences in dose rates

The ratios of the dose rates of the detectors to those of the laterally set TCS-161 are presented in Table 5 together with the averaged values. The averaged ratios are 1.14 for C12137-00, 0.83 for C12137-01 and 1.06 for GR1. The result of C12137-00 is slightly overestimated, that of C12137-01 seem underestimated and that of GR1 agrees with that of TCS-161 within uncertainties.

With regard to C12137-10 and Falcon 5000, the ratios at Nos. 2 and 5 are much higher than those obtained at the other locations. These overestimations would be because of insufficient counting loss correction for the data measured where the $H^*(10)$ rates exceeded 2 μSv/h. Therefore, excluding the results from Nos. 2 and 5 from the following discussions, the averaged ratios are 0.83 for C12137-10 in the lateral setting, 0.77 for C12137-10 in the upward setting and 1.22 for Falcon 5000.

Although the result of Falcon 5000 agrees with that of TCS-161 within uncertainties, the results of C12137-10 are underestimated.

$G(E)$ functions

Table 6 shows the dose rates obtained using the $G(E)$ functions determined in ROT. Each ratio of dose rate to that of TCS-161 in the lateral setting is presented in Table 7. The averaged ratios of the dose rates obtained using the $G(E)$ functions in AP are changed as follows: C12137-00 (1.14⟶1.05), C12137-01 (0.83⟶0.95), C12137-10 (0.83⟶1.00, lateral setting), C12137-10 (0.77⟶1.67, upward setting) and GR1 (1.06⟶1.12). Although the result of GR1 is slightly even worse due to its cubic crystal shape, in other cases the agreement of $H^*(10)$ rates with that of TCS-161 is improved, except for C12137-10 measured in the upward position.

For C12137-10 in the lateral setting, the dose rates agree with those of TCS-161 on average. These results indicate that ROT enables better approximation of the gamma-ray incidence direction in the environment than AP.

Figure 6 presents the ratios of the $G(E)$ functions determined in AP to those in ROT. In the case of TCS-161, for example, the ratios are fairly close to unity in the whole range of the pulse height due to its relatively small directional dependence. For C12137-00, although the ratio is almost unity in most of the pulse height regions, the ratios increase by +40% at the maximum at pulse heights below 300 keV.

However, about the results of C12137-10 measured in the upward position, the ratios are almost between 0.3 and 0.6; that is, the $G(E)$ functions for ROT are much larger than those in AP because of its relatively small effective crystal surface in ROT. As a result, the dose rates are 1.67 times higher than those of TCS-161 on average, as shown in Table 7. This result

Downloaded from https://academic.oup.com/rpd/article/193/3-4/228/6248462 by Japan Atomic Energy Agency user on 16 August 2021

Table 6. $H^*(10)$ rates in μSv/h using $G(E)$ functions in ROT geometry.

Place	C12137-00	C12137-01	TCS-161	C12137-10		GR1
			(lat.)	lat.	up	
No.1	0.231	0.230	0.224	0.218	0.384	0.254
No.2	2.406	1.995	2.191	3.485	5.716	2.595
No.3	0.206	0.190	0.199	0.188	0.313	0.204
No.4	0.629	0.576	0.600	0.638	1.059	0.679
No.5	2.707	2.148	2.369	3.724	6.004	3.039
No.6	0.209	0.213	0.228	0.222	0.375	0.221

Table 7. Ratios of $H^*(10)$ rate of TCS-161 (lat.) to those of other detectors, using $G(E)$ functions for ROT geometry.

Place	C12137	C12137	C12137-10		GR1
	-00	-01	lat.	up.	
No.1	1.03	1.03	0.97	1.71	1.13
No.2	1.10	0.91	(1.59)	(2.61)	1.18
No.3	1.04	0.96	0.94	1.58	1.03
No.4	1.05	0.96	1.06	1.77	1.13
No.5	1.14	0.91	(1.57)	(2.53)	1.28
No.6	0.92	0.93	0.97	1.64	0.97
Average	1.05	0.95	1.00*	1.67*	1.12
	±0.07	±0.04	±0.05	±0.07	±0.10

*The values of no.2 and no.5 are not included.

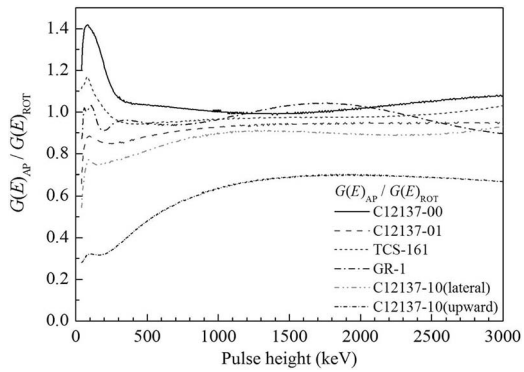

Figure 6: Ratios of the G(E) functions determined in anterior–posterior irradiation geometry (AP) to those in rotational irradiation geometry (ROT).

reveals the limitation of the replacement of $G(E)$ functions in ROT with those in AP and the necessity of scintillation detectors with low directional dependence in environmental dose rate monitoring.

CONCLUSIONS

$H^*(10)$ rates were measured with several different detectors where radioactive caesium isotopes exist in the soil in Fukushima. Differences were observed in the indicated values of $H^*(10)$. Such variation is attributed to the directional dependence of the detectors used and could be mostly compensated using $G(E)$ functions determined in ROT. However, one can conclude from the results of C12137-10, which has an extremely flat crystal configuration that scintillation detectors with low directional dependence are required for environmental dose rate monitoring, given that even replacement of $G(E)$ functions with those for ROT could not completely compensate directional dependence in any crystal configuration. Lateral usage of C12137-10 is useful, but detector settings cannot always be considered, especially under accident conditions. Further investigation will be needed in terms of crystal configurations suitable for environmental dose rate measurement.

ACKNOWLEDGEMENTS

The authors are grateful to Messrs. Y. Ebata and Y. Sato from Institute of radiation measurements, Mr A. Yoshida from Hitachi, Ltd and Drs T. Abe, K. Hoshi, and Mr A. Nidaira from the Radiation Safety and Control sections in JAEA for energy calibration of the scintillation detectors. We also thank Drs M. Andoh, S. Mikami from Sector of Nuclear Safety

Downloaded from https://academic.oup.com/rpd/article/193/3-4/228/6248462 by Japan Atomic Energy Agency user on 16 August 2021

Research and Emergency Preparedness of JAEA, and Dr Y. Tanimura from the Radiation Safety and Control section of JAEA for measurement in Fukushima prefecture.

FUNDING

Japan Atomic Energy Agency and the Nuclear Regulation Authority (No. 16040167).

REFERENCES

1. CS (Cabinet Secretariat), Final Report of the Investigation Committee on the Accident at the Fukushima Nuclear Power Stations of Tokyo Electric Power Company, Tokyo, Japan: Cabinet Secretariat. http://www.cas.go.jp/jp/seisaku/icanps/eng/final-report.html (2012) (accessed 14 April 2021).
2. Tanigaki, M., Okumura, R., Takamiya, K., Sato, N., Yoshino, H. and Yamana, H. *Development of a car-borne γ-ray survey system, KURAMA*. Nucl. Instr. and Meth. **A726**, 162–168 (2013).
3. Hamamatsu Photonics K.K. Radiation detection module C12137. (Hamamatsu, Japan: Hamamatsu Photonics K.K.). https://www.hamamatsu.com/jp/ja/product/optical-sensors/radiation-sensor/radiation-detection-module/index.html (accessed 14 April 2021).
4. Horiba Ltd., PA-1000 Environmental Radiation Monitor Radi, (Tokyo: Horiba Ltd.). http://www.horiba.com/uk/process-environmental/products/environmental-radiation-monitor/details/pa-1000-environmental-radiation-monitor-radi-3124/, (accessed 14 April 2021).
5. Sekiya Rika Co., Ltd, Mr.Gamma, A2700. (Tokyo:Sekiya Rika Co., Ltd), http://www.sekiyarika.com/labo-ware/chemical-apparatus/products/A2700/Gamma_A2700.html, (accessed 14 April 2021).
6. Tanigaki, M., Okumura, R., Takamiya, K., Sato, N., Yoshino, H., Yoshinaga, H., Kobayashi, Y., Uehara, A. and Yamana, H. *Development of KURAMA-II and its operation in Fukushima*. Nucl. Instr. and Meth. **A781**, 57–64 (2015).
7. Tsuda, S. *et al. Construction of a car-borne survey system for measurement of dose rates in air: KURAMA-II, and its application*. JAEA-Technology 2013-037 (in Japanese) (2013).
8. Tsuda, S., Yoshida, T., Tsutsumi, M. and Saito, K. *Characteristics and verification of a car-borne survey system for dose rates in air: KURAMA-II*. J. Environ. Radioact. **139**, 260–265 (2015).
9. Moriuchi, S. and Miyanaga, I. *A spectrometric method for measurement of low-level gamma exposure dose*. Health Phys. **12**, 541–551 (1966).
10. Tsuda, S. and Saito, K. *Spectrum-dose conversion operator of NaI(Tl) and CsI(Tl) scintillation detectors for air dose rate measurements in contaminated environments*. J. Environ. Radioact. **166**, 419–426 (2017).
11. Tsuda, S., Tanigaki, M., Yoshida, T., Okumura, R. and Saito, K. *Dependence of crystal configuration of scintillation detectors on dose rate 5 measurement in the environment*. Trans. At. Energy Soc. Jpn. **17**, 11–17 (2018). doi: 10.3327/taesj.J16.039 [in Japanese].
12. Radiation Safety Associates, "URSA II" (English), http://www.radpro.com/product/ursa-ii/, (accessed 14 April 2021).
13. Kromek Group plc. GR1-A® and GR1®. (Kromek Group plc.), Durham, UK. https://www.kromek.com/images/products/GR1USLRev12.pdf, (accessed 14 April 2021).
14. Mikami, S. *et al. Spatial distributions of radionuclides deposited onto ground soil around the Fukushima Daiichi Nuclear Power Plant and their temporal change until December 2012*. J. Environ. Radioact. **139**, 320–343 (2015).
15. Mirion Technologies, Inc. Falcon 5000® Portable HPGe-Based Radionuclide Identifier. (USA: Mirion Technologies, Inc.) https://www.canberra.com/fr/produits/hp_radioprotection/falcon-5000.html, (accessed 14 April 2021).
16. Tsuda, S. and Tsutsumi, M. *Calculation and verification of the spectrum - dose conversion operator of various CsI(Tl) scintillation counters for gamma-ray*. Jpn. J. Health Phys. **47**(4), 260–265(in Japanese) (2012).
17. ICRP. *Conversion coefficients for use in radiological protection against external radiation.* ICRP publication 74. Ann. ICRP **26**(3–4) (1996).
18. Sato, T. *et al. Particle and heavy ion transport code system PHITS, version 2.52*. J. Nucl. Sci. Technol. **50**, 913–923 (2013).
19. Saito, K. and Petoussi-Henss, N. P. *Ambient dose equivalent conversion coefficients for radionuclides exponentially distributed in the ground*. J. Nucl. Sci. Technol. **51**(10), 1274–1287 (2014).
20. ICRU. Gamma-Ray Spectrometry in the Environment ICRU Report 53. (Bethesda, MD: ICRU) (1994).
21. Japan Atomic Energy Agency, Database for Radioactive Substance Monitoring Data. (Ibaraki, Japan: Japan Atomic Energy Agency). https://emdb.jaea.go.jp/emdb/en/, (accessed 14 April 2021).
22. Saito, K., Petoussi-Henss, N. and Zankl, M. *Calculation of the effective dose and its variation from environmental gamma ray sources*. Health Phys. **74**, 698–706 (1998).

Downloaded from https://academic.oup.com/rpd/article/193/3-4/228/6248462 by Japan Atomic Energy Agency user on 16 August 2021